ACS APPLIED MATERIALS & INTERFACES

Research Article

www.acsami.org

Controlling Number of Indene Solubilizing Groups in Multiadduct Fullerenes for Tuning Optoelectronic Properties and Open-Circuit Voltage in Organic Solar Cells

Hyunbum Kang,[†,‡] Chul-Hee Cho,[†,‡] Han-Hee Cho,[†] Tae Eui Kang,[†] Hyeong Jun Kim,[†] Ki-Hyun Kim,[†] Sung Cheol Yoon,*[,§] and Bumjoon J. Kim*[,†]

[†]Department of Chemical & Biomolecular Engineering, Korea Advanced Institute Science and Technology (KAIST), Daejeon 305-701, Korea

[§]Advanced Materials Division, Korea Research Institute of Chemical Technology (KRICT), Daejeon 305-600, Korea

Supporting Information

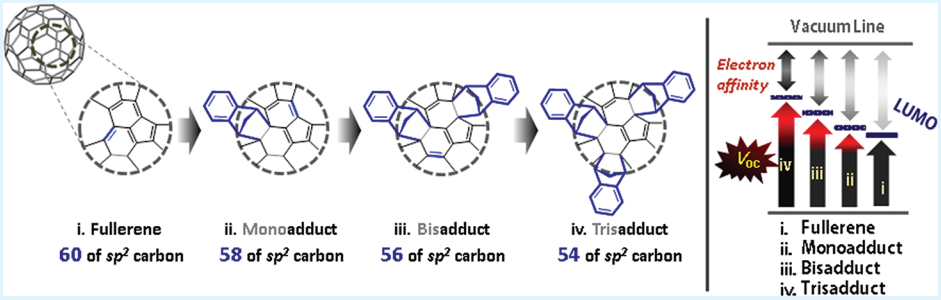

ABSTRACT: The ability to tune the lowest unoccupied molecular orbital (LUMO)/highest occupied molecular orbital (HOMO) levels of fullerene derivatives used as electron acceptors is crucial in controlling the optical/electrochemical properties of these materials and the open circuit voltage (V_{oc}) of solar cells. Here, we report a series of indene fullerene multiadducts (ICMA, ICBA, and ICTA) in which different numbers of indene solubilizing groups are attached to the fullerene molecule. The addition of indene units to fullerene raised its LUMO and HOMO levels, resulting in higher V_{oc} values in the photovoltaic device. Bulk-heterojunction (BHJ) solar cells fabricated from poly(3-hexylthiophene) (P3HT) and a series of fullerene multiadducts-ICMA, ICBA, and ICTA showed V_{oc} values of 0.65, 0.83, and 0.92 V, respectively. Despite demonstrating the highest V_{oc} value, the P3HT:ICTA device exhibited lower efficiency (1.56%) than the P3HT:ICBA device (5.26%) because of its lower fill factor and current. This result could be explained by the lower light absorption and electron mobility of the P3HT:ICTA device, suggesting that there is an optimal number of the solubilizing group that can be added to the fullerene molecule. The effects of the addition of solubilizing groups on the optoelectrical properties of fullerene derivatives were carefully investigated to elucidate the molecular structure−device function relationship.

KEYWORDS: *multiadduct fullerenese, electron acceptors , lowest unoccupied molecular orbital (LUMO), open circuit voltage (V_{oc}), polymer solar cells (PSCs)*

INTRODUCTION

Polymer solar cells (PSCs) based on conjugated polymers and fullerene derivatives have attracted a great deal of attention because of their mechanical flexibility, simple fabrication process, and the potential for their low-cost, large-scale manufacture.[1−4] Until now, one of the most representative polymer donors and fullerene derivative acceptors used in polymer solar cells has been regioregular poly(3-hexylthiophene) (P3HT) and [6,6]-phenyl-C_{61}-butyric acid methyl ester (PCBM), respectively. PSCs based on the P3HT/PCBM BHJ have reproducibly reached power conversion efficiencies (PCEs) greater than 4% by solvent annealing as well as thermal annealing.[5−8] And research activities on development of new materials have been intensively focused on new low-bandgap p-type materials in order to extend the light absorption to 900 nm and increase light harvesting; these polymers produce high efficiencies greater than 7%.[9−17] However, many of the reported conjugated polymers, including P3HT, suffer from low efficiency in photovoltaics because of a loss of V_{oc}.[18−20] The use of PCBM, which has a relatively low LUMO level, limits the V_{oc} of the PSCs because V_{oc} is proportional to the difference between the LUMO of the acceptor and the HOMO of the donor material.[21]

To overcome this problem, a number of fullerene derivatives with high LUMO levels have recently designed and synthesized for use as electron acceptors in high-V_{oc} PSCs.[22−26] For

Received: August 11, 2011
Accepted: December 12, 2011
Published: December 12, 2011

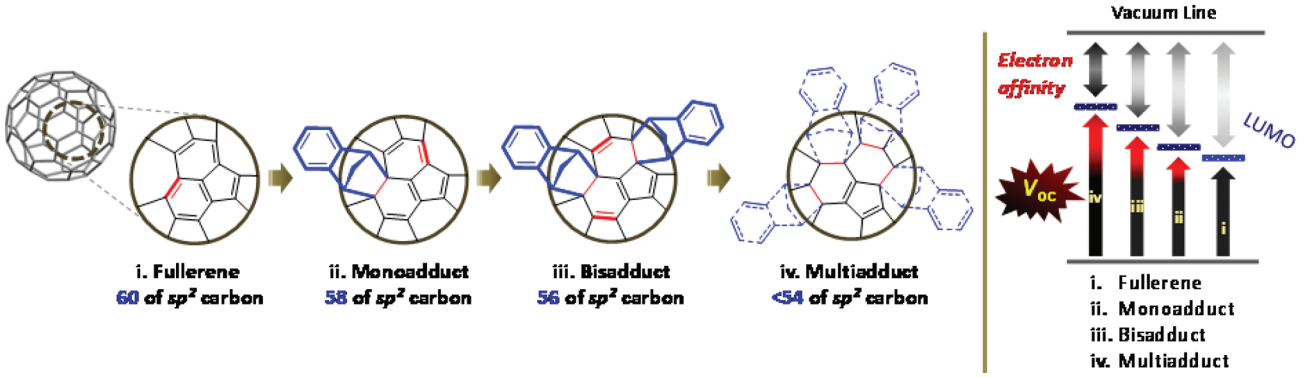

Figure 1. Schematic illustration of mono-, bis-, and multiadduct fullerenes with different number of the solubilizing groups (left). The schematic presents the resulting change in the LUMO levels of the fullerenes as a function of the number of the solubilizing groups (right).

example, the use of a regioisomeric mixture of PCBM bisadduct (bis-PCBM) isomers was reported by Blom et al.[22] LUMO energy level of bis-PCBM is approximately 0.1 eV higher than that of PCBM, and the PCE of a PSC based on P3HT and bis-PCBM reached 4.5%, which constitutes an 18% increase over the PCE achieved with PCBM. This increase is a result of the higher V_{oc} (0.73 V) caused by the higher LUMO energy level.[22] More recently, Laird[27] and Li et al.[28−30] reported a remarkable bisadduct fullerene derivative, indene-C_{60} bisadduct (ICBA). Through Diels−Alder [4 + 2] cycloaddition of indene to the C_{60} fullerene structure, ICBA achieves a LUMO energy level that is 0.17 eV higher than that of single-functionalized PCBM. A PSC based on P3HT using ICBA as an acceptor demonstrated a V_{oc} of 0.84 V and a PCE of greater than 5.44%, whereas a cell based on P3HT/PCBM displayed a V_{oc} of 0.6 V and a PCE of 3.88% under the same experimental conditions.[28] Thus, the development of new fullerene derivatives with tunable LUMO and HOMO levels is both urgent and important.

The standard fullerene acceptor contains 60 sp^2 orbitals, of which fullerene derivatives with solubilizing groups have a reduced number. For example, the monoadduct has 58 sp^2 orbitals and the bisadduct has 56 sp^2 orbitals. The electron affinity of bisadduct fullerene is lower than that of the monoadduct because of the difference in the sp^2 orbital number (Figure 1).

The multiadduct contains fewer sp^2 carbons, reducing the electron affinity; thus, it displays a high LUMO energy level. Therefore, it is expected that a further increase in the number of the solubilizing groups (i.e., trisadduct fullerene) will result in further reduced electron affinity and the potential for a higher value of V_{oc}. Recently, Blom,[24] Nelson,[31] and Fukuzumi et al.[32] reported a series of PCBM-based multiadducts. However, it was found that multiadducts of tris- and tetrakis-PCBM blended with P3HT produced very low efficiencies in BHJ devices. In addition, the V_{oc} values of P3HT:multiadduct based BHJ devices were not typically higher than those of bis-PCBM based BHJ devices. Additionally, whereas indene-based fullerenes have shown great potential as electron acceptors, there have been no reports of the use of trisadduct indene-based fullerene (ICTA) as the electron acceptor in PSCs, to the best of our knowledge.

Here, we report the synthesis of a series of indene-C_{60} multiadducts including indene-C_{60} monoadduct (ICMA), indene-C_{60} bisadduct (ICBA), and indene-C_{60} trisadduct (ICTA) with different numbers of indene solubilizing groups, ranging from 1 to 3. We have investigated the effects of the number of solubilizing groups added to the fullerene on its electrochemical and optical properties. And we have studied the correlation of LUMO and V_{oc} in BHJ solar cells. The LUMO levels of ICMA, ICBA and ICTA were found to be −3.84, −3.67, and −3.53 eV, respectively, indicating that an increase in the number of solubilizing groups increased the LUMO levels of the compounds. As a result, BHJ devices consisting of P3HT:ICMA, P3HT:ICBA and P3HT:ICTA demonstrated increased V_{oc} values of 0.65, 0.83, and 0.92 V, respectively. Interestingly, the P3HT:ICTA BHJ device displayed one of the highest V_{oc} values that have been reported for P3HT-based solar cells. However, because of its lower current and fill factor, this device demonstrated a lower PCE (1.56%) than P3HT:ICBA (5.26%). To better understand this result, we will discuss the effects of the addition of solubilizing groups to the fullerene molecule on the charge mobility as well as the optical and morphological properties of its blend with P3HT.

EXPERIMENTAL SECTION

Synthesis of Indene C_{60} Multiadducts (Monoadduct, Bisadduct, and Trisadduct). The compounds were prepared using a modification of a published procedure.[33] C_{60} (500 mg, 0.695 mmol) and indene (970 mg, 8.34 mmol) were dissolved in dry 1,2-dichlorobenzene (35 mL) at reflux temperature for 60 h under an argon atmosphere. Upon cooling to room temperature, the reaction mixture was precipitated with excess MeOH. After the cosolvent was removed with filter paper, the combined crude solid product was purified using column chromatography on silica gel with toluene/hexanes as the gradient eluent. This separation yielded corresponding products, such as ICBA (272 mg, 41%, brown solid) and ICTA (171 mg, 23%, brown solid). In contrast, ICMA gave only trace yields.

ICBA. Elemental anal. Calcd for $C_{78}H_{16}$: C, 98.3; H, 1.7. Found: C, 97.1; H, 1.7. MALDI-TOF MS: calcd for $C_{78}H_{16}$, 952.962; found, 953.069 (M^+). ICTA. Elemental anal. Calcd for $C_{87}H_{24}$: C 97.7; H, 2.3. Found: C, 96.3; H, 2.0. MALDI-TOF MS: calcd for $C_{87}H_{24}$, 1069.121; found, 1069.249 (M^+).

When 2.0 equiv. of indene was used, C_{60} (0.5 g, 0.695 mmol) in dry 1,2-dichlorobenzene (35 mL) was refluxed for 48 h with indene, and the following indene C_{60} monoadduct (186 mg, 32%, brown solid) product was obtained. ICMA. ^{1}H NMR (400 MHz, $CDCl_3$): δ 7.61−7.65 (m, 2H), 7.42−7.46 (m, 2H), 4.95 (br s, 2H), 3.85 (dt, J = 10.2, 1.6 Hz, 1H), 2.92 (dt, J = 10.2, 1.6 Hz, 1H). elemental anal. Calcd for $C_{69}H_8$: C, 99.0; H, 1.0. Found: C, 97.4; H, 1.2. MALDI-TOF MS: calcd for $C_{69}H_8$, 836.802; found, 836.983 (M^+).

Characterization Methods. UV−visible absorption spectra were obtained using a JASCO V-570 spectrophotometer. Cyclic voltammetry (CV) curves were measured using a CHI 600C electrochemical analyzer. The CV curves of the different electron acceptors (PCBM, ICMA, ICBA and ICTA) were collected at room temperature using a conventional three-electrode system (Pt disk working electrode, Pt

dx.doi.org/10.1021/am201075y | ACS Appl. Mater. Interfaces 2012, 4, 110−116

Scheme 1. Synthesis of Indene C_{60} multiadducts (ICMA, ICBA, and ICTA)

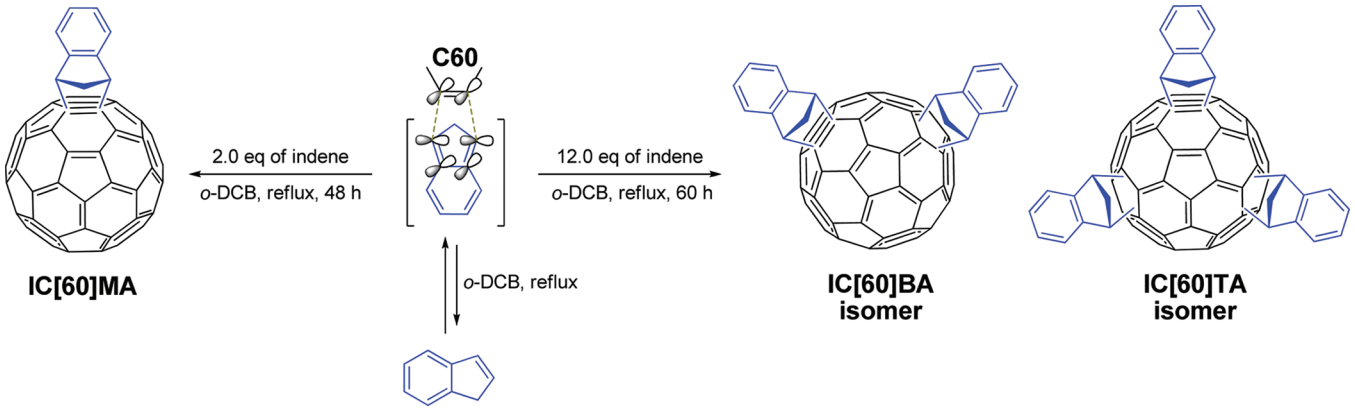

wire counter-electrode and Ag wire quasi-reference electrode) in 0.1 M tetrabutylammonium hexafluorophosphate (n-Bu_4PF_6) solution in 1,2-dichlorobenzene (o-DCB) at a potential scan rate of 10 mV/s. The reduction potentials of the acceptor solutions against the Ag quasi-reference electrode were measured and calibrated against a ferrocene/ferrocenium (Fc/Fc^+) redox couple, assuming that the absolute energy level of Fc/Fc^+ was −4.80 eV.[14,31,32]

Device Fabrication and Measurement. To investigate the photovoltaic properties of the indene fullerene multiadducts, BHJ photovoltaic cells were fabricated using an ITO/PEDOT:PSS/P3HT:Electron acceptors/LiF/Al structure. P3HT (BASF P200) was used as an electron donor, while PCBM, ICMA, ICBA, and ICTA were used as electron acceptors. ITO-coated glass substrates were subjected to ultrasonication in acetone and 2% Helmanex soap in water, followed by extensive rinsing with deionized water and ultrasonication in deionized water and then in isopropyl alcohol. Finally, the substrates were dried for several hours in an oven at 80 °C. The ITO substrates were treated with UV-ozone prior to PEDOT:PSS deposition. A filtered dispersion of PEDOT:PSS in water (PH 500) was applied by spin-coating at 3000 rpm for 30 s and baking for 30 min at 140 °C in air. After application of the PEDOT:PSS layer, all subsequent procedures were performed in a glovebox under a N_2 atmosphere. Different solutions of P3HT, PCBM, ICMA, ICBA, and ICTA in o-dichlorobenzene (30 mg/mL) were prepared and stirred at 100 °C for more than 24 h. The solutions were passed through a 0.2 μm PTFE syringe filter. Then, blend solutions composed of P3HT mixed with PCBM, ICMA, ICBA and ICTA were prepared with a P3HT concentration of 15 mg/mL. Each solution was then spin-cast onto an ITO/PEDOT:PSS substrate at 800 rpm. Each P3HT/acceptor film was placed in a covered Petri dish while still wet for the solvent annealing process. Before the deposition of LiF/Al, prethermal annealing was performed at 150 °C for 10 min to optimize the morphology of the active layer. The substrates were then placed in an evaporation chamber and held under high vacuum <1×10^{-6} Torr) for more than 1 h before evaporating approximately 0.7 nm of LiF/100 nm of Al. The configuration of the shadow mask produced four independent devices on each substrate. The photovoltaic performance of the devices was characterized with a solar simulator (ABET Technologies) with an air-mass (AM) 1.5 G filter. The intensity of the solar simulator was carefully calibrated using an AIST-certified silicon photodiode. The current−voltage behavior was measured using a Keithley 2400 SMU. The active area of the fabricated devices was 0.10 cm^2.

The hole mobilities of the P3HT used as an electron donor in the blended systems were measured by the space-charge-limited current (SCLC) method using the ITO/PEDOT:PSS/blend/Au device structure. Current−voltage measurements in the range of 0−8 V were taken, and the results were fitted to a space-charge-limited function. The SCLC is described by

$$J_{SCLC} = \frac{9}{8}\varepsilon\varepsilon_0\mu\frac{V^2}{L^3}$$

where ε_0 is the permittivity of free space, ε is the dielectric constant of the polymer, μ is the mobility of the charge carriers, V is the potential across the device ($V = V_{applied} - V_{bi} - V_r$), and L is the polymer layer thickness. The series and contact resistances of the device (~25 Ω) were measured using a blank device (ITO/PEDOT/Au), and the voltage drop caused by this resistance (V_r) was subtracted from the applied voltage. Electron-only devices with the structure ITO/CS_2CO_3/blend/LiF/Al were also fabricated by spin-coating the active layer onto ITO/CS_2CO_3 substrates followed by the deposition of LiF/Al on the cathode electrode, as reported in the literature.[34]

RESULTS AND DISCUSSION

Synthesis. A series of indene-C_{60} multiadducts of ICMA, ICBA and ICTA were synthesized using the [4 + 2] cycloaddition reaction between C_{60}-fullerene and diene, as outlined in Scheme 1. Although the compounds were prepared using a modification of a published procedure,[28,33] the synthesis of ICTA with three indene solubilizing groups and the analysis of its chemical structure have not previously been reported in the literature. The relative weight ratios of ICMA, ICBA and ICTA in the product mixtures were dependent on the reaction conditions, including the molar ratios of indene to C_{60} and the reaction times used. Despite the use of an extended reaction time and a greater excess of indene, higher-adduct products (e.g., tetrakis- and pentakisadducts) could not be obtained using this reaction procedure.

When 12.0 equiv of indene was used, the crude products were mixtures of indene C_{60} multiadducts (such as ICBA, ICTA, and a small amount of ICMA) and unreacted C_{60}. The solvent, o-DCB, was partially evaporated under reduced pressure. The desired products, ICBA (41%) and ICTA (23%), were separated and purified using column chromatography (hexane/toluene eluent gradient system). The structures of ICBA and ICTA were confirmed using MALDI-TOF mass spectrometry and elemental analysis. When 2.0 equiv of indene was used, the cycloaddition product, (the C_{60} monoadduct, ICMA), was obtained in an isolated yield of 32% (based on C_{60} fullerene) together with a small amount of ICBA and unreacted C_{60}. The purities of the ICMA, ICBA and ICTA products were analyzed using elemental analysis and MALDI-TOF mass spectroscopy (see Figures S1−S3 in the Supporting Information) and were determined to be greater than 99%.

Electrochemical Properties. The LUMO/HOMO levels of fullerene derivatives are of great importance in determining

the potential of these compounds as electron acceptors in photovoltaic cells. The electrochemical properties of a series of indene-fullerene multiadducts were therefore carefully analyzed using CV measurements. The CV curves were recorded with referenced to a Ag quasi-reference electrode, which was calibrated using a ferrocene/ferrocenium (Fc/Fc^+) redox couple (4.80 eV below the vacuum level) as an external standard.[14,35,36]

Figure 2 shows the CV curves of ICMA, ICBA, and ICTA along with that of PCBM for comparison. Table 1 summarizes

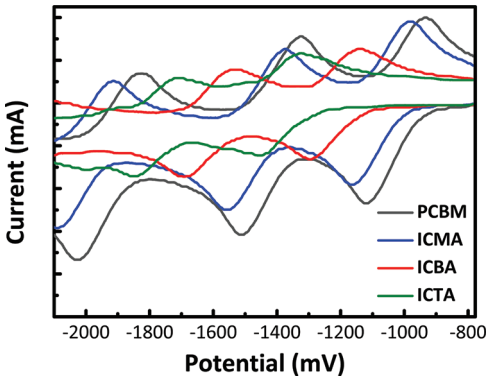

Figure 2. Cyclic voltammetry (CV) curves for PCBM, ICMA, ICBA, and ICTA.

Table 1. Electrochemical Properties of the Series of Indene-Fullerene Multiadducts Used in This Study

electron acceptors	E_1 (V)	E_2 (V)	E_{red}^{on} (V)	LUMO (eV)
PCBM	−1.11	−1.51	−0.95	−3.85
ICMA	−1.15	−1.55	−0.96	−3.84
ICBA	−1.29	−1.69	−1.13	−3.67
ICTA	−1.44	−1.85	−1.27	−3.53

the electrochemical properties of the fullerene materials used in our study. The series of indene−fullerene multiadducts and PCBM exhibit two well-defined, quasi-reversible reduction waves in the negative potential range from 0 to −2.5 V.

As shown in Figure 2 and Table 1, the first (E_1) and second (E_2) reduction potentials decreased as the number of solubilizing groups in the fullerenes increased; the most negatively shifted values were those observed for ICTA, which has the largest number of indene units among the electron-accepting fullerenes used. Compared to the E_1 of ICMA (−1.15 V), the E_1 of ICBA is shifted by −0.14 V, to −1.29 V, and that of ICTA is shifted by −0.29 V, to −1.44 V. The LUMO energy levels of the fullerene derivatives were estimated from their onset reduction potentials, which were determined by CV measurements. The onset reduction potentials (E_{red}^{on}) of PCBM, ICMA, ICBA, and ICTA were −0.95, −0.96, −1.13, and −1.27 V, respectively, vs Fc/Fc^+. As shown in Table 1, whereas ICMA has a LUMO level very similar to that of PCBM, the indene-fullerene bis- and trisadducts ICBA and ICTA exhibit much higher LUMO levels than the monoadduct fullerenes PCBM and ICMA. For example, the LUMO level of ICBA is −3.67 eV, a value that is 0.17 eV higher than that of ICMA. This trend is consistent with previously reported findings.[28] Of particular interest is the observation that the LUMO level of ICTA is −3.53 eV, a value that is higher than that of ICBA by 0.14 eV. The large shift in the LUMO level of ICTA is attributed to the presence of an extra indene group and the resulting decrease in the sp^2 orbital number (the bisadduct has 56 sp^2 orbitals, whereas the trisadduct has 54 sp^2 orbitals) and electron affinity. The higher LUMO energy level of the indene-fullerene multiadduct derivatives is desirable because electron acceptors of this type produce higher values of V_{oc} in BHJ-type PSCs. This topic will be discussed further in the following section.

Photovoltaic Properties. To elucidate the relationship between the molecular structure of indene-fullerene multiadducts and the function of solar cell devices, BHJ-type PSCs (ITO/PEDOT:PSS/P3HT:indene-fullerene multiadducts/LiF/Al) were fabricated from blends of these fullerenes with P3HT, and their performances were measured. A device composed of P3HT:PCBM was also fabricated as a control. Solvent annealing was used to optimize the morphology of the BHJ active layer and improve the device performance via control over the evaporation rate of the residual solvent. Figure 3a

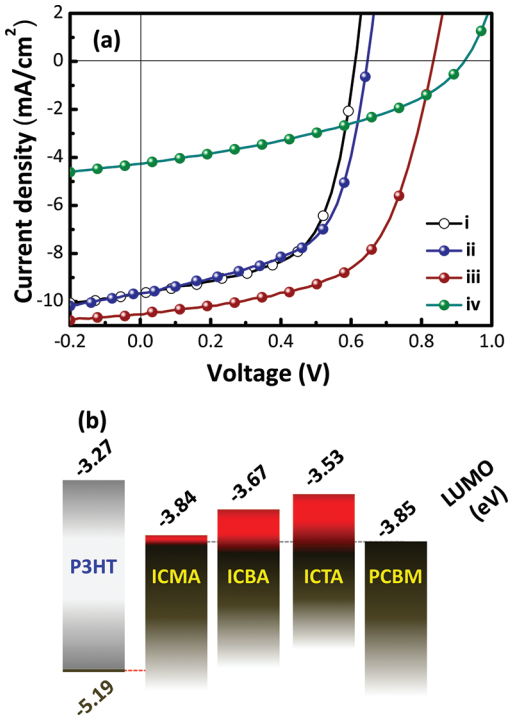

Figure 3. (a) Current density−voltage characteristics of BHJ-type PSCs; (i) P3HT:PCBM (black), (ii) P3HT:ICMA (blue), (iii) P3HT:ICBA (red), and (iv) P3HT:ICTA (green) based BHJ devices under AM 1.5 illumination at 100 mW/cm^2. (b) Energy-band diagram showing the LUMO levels of the indene C_{60} multiadducts studied (ICMA, ICBA, and ICTA).

shows the current density versus voltage ($J-V$) curves of the ITO/PEDOT:PSS/P3HT:indene-fullerene multiadduct/LiF/Al devices under AM 1.5 illumination at 100 mW/cm^2. Table 2 summarizes the device characteristics of the P3HT-based BHJ-type PSCs mixed using different weight ratios of PCBM, ICMA, ICBA and ICTA. The P3HT:ICMA device exhibited a PCE of 3.65% (V_{oc} = 0.65 V, J_{sc} = 9.66 mA/cm^2, and FF = 0.59) at a P3HT:ICMA weight ratio of 50:50, and its performance was comparable to that of the P3HT:PCBM control device (V_{oc} = 0.61 V, J_{sc} = 9.68 mA/cm^2, FF = 0.61, and PCE = 3.59%) .

Interestingly, the P3HT:ICBA device performed much better (V_{oc} = 0.83 V, J_{sc} = 10.53 mA/cm^2, FF = 0.60, and PCE =

dx.doi.org/10.1021/am201075y | ACS Appl. Mater. Interfaces 2012, 4, 110−116

Table 2. Device Characteristics of Solar Cells Composed of P3HT:ICMA, P3HT:ICBA, and P3HT:ICTA along with P3HT:PCBM under AM 1.5 G-Simulated Solar Illumination (100 mW/cm^2)

active layer (w/w)	V_{oc} (V)	J_{sc} (mA/cm^{-2})	FF	PCE (%)
P3HT: PCBM (60:40)	0.62	9.71	0.62	3.74
P3HT: PCBM (50:50)	0.61	9.68	0.61	3.59
P3HT: ICMA (60:40)	0.63	9.25	0.60	3.46
P3HT: ICMA (50:50)	0.65	9.66	0.59	3.65
P3HT: ICBA (60:40)	0.83	10.53	0.60	5.26
P3HT: ICBA (50:50)	0.83	10.45	0.59	5.10
P3HT: ICTA (60:40)	0.88	6.27	0.40	2.25
P3HT: ICTA (50:50)	0.92	4.26	0.40	1.56

5.26%) than the devices based on blends of P3HT and the monoadduct fullerenes (PCBM and ICMA) at various donor:acceptor weight ratios. The increase in the PCE of the P3HT:ICBA device was mainly caused by an increase in V_{oc} (its value increased by 0.18 V compared to that of the P3HT:ICMA device). The changes in the V_{oc} value and the device performance observed in this study agree well with previously reported values.[28,30] The use of ICTA as an electron acceptor produced a further increase in V_{oc} to more than 0.9 V. To the best of our knowledge, this is one of the highest V_{oc} reported to date for a polythiophene based BHJ-type PSC. However, despite its high V_{oc} value, the P3HT:ICTA device exhibited lower performance (V_{oc} = 0.92 V, J_{sc} = 4.26 mA/cm^2, FF = 0.40, and PCE = 1.56%) than the P3HT:ICBA device (5.26%). BHJ devices consisting of P3HT:ICMA, P3HT:ICBA and P3HT:ICTA, in order of increasing number of indene solubilizing groups added to the fullerene, exhibited increased V_{oc} values of 0.65, 0.83, and 0.92 V, respectively. This trend can be explained by considering an energy-band diagram of the fullerenes and P3HT used in our study (Figure 3b). It is well-known that V_{oc} is mainly determined by the difference between the LUMO level of the electron acceptor and the HOMO level of the electron donor, although other factors such as device morphology and charge mobility make minor contributions.[37] The increase in the LUMO levels of ICMA, ICBA and ICTA with increasing side chain number (−3.84, −3.67, and −3.53 eV, respectively) results in increasing gaps between the LUMO level of each fullerene and the HOMO level of P3HT. Thus, it can be concluded that the progressive addition of solubilizing groups to the fullerene results in significant increases in the value of V_{oc}. Although the P3HT:ICTA device had a higher V_{oc} than the P3HT:ICMA and P3HT:ICBA devices, this device produced a much lower current and fill factor than the P3HT:ICMA and ICBA devices. The optical and electrical properties of ICMA, ICBA and ICTA devices will be discussed in the following section to elucidate the reason for the lower current and fill factor values in the ICTA device.

Optical and Electrical properties. To gain insight into the operation of BHJ solar cells, the thin-film UV−vis absorption spectra of the P3HT:fullerene blends were measured under the optimal conditions for each device, as shown in Figure 4. The UV−vis absorption spectra of P3HT:PCBM and P3HT:ICMA were similar to that of a pristine P3HT film, with a λ_{max} of 517 nm. P3HT:ICBA showed a slightly hypsochromic-shifted spectrum (λ_{max} = 510 nm) compared to that of the pristine P3HT films. P3HT:ICTA showed a dramatic change in the absorption spectrum, with a much stronger hypsochromic shift (λ_{max} = 487 nm).

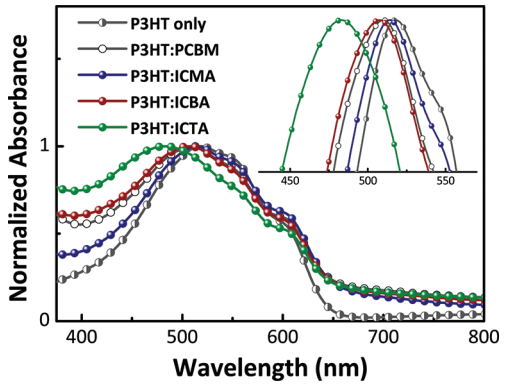

Figure 4. UV−vis absorption spectra of thin films of PCBM, ICMA, ICBA, and ICTA with P3HT.

Furthermore, the optical spectra of the P3HT:ICTA films exhibited decreased intensity of the vibronic peak at 610 nm, which is characteristic of highly ordered P3HT chains.[5,38−40] We suspect that the addition of solubilizing groups to the fullerenes may introduce disorder into the fullerene packing because of the presence of a higher number of isomers in ICTA that can disrupt the two-dimensional packing between the electron-donating polymers and their consequent crystallization. A previous study reported a similar UV−vis absorption trend in blended films of P3HT:bis-PCBM in comparison to P3HT:PCBM.[41] To find the additional evidence of the effect of the fullerene molecular structure on the P3HT packing in the P3HT:multiadduct blend films, the two-dimensional structure of the P3HT chains and their orientation is under investigation by grazing incidence X-ray diffraction (GIXRD) and high-resolution X-ray scattering.

Charge-carrier mobility is of great importance in PSCs. The space-charge-limited current (SCLC) mobility measures the hole and electron mobility in the direction perpendicular to the electrodes; thus, it is the most representative measurement of charge-carrier mobility for solar cells. To measure the hole mobility of different fullerene blends with P3HT, we fabricated devices with the ITO/PEDOT:PSS/blend/Au structure, resulting in a hole-only device. For blends of ICMA, ICBA and ICTA with P3HT prepared using this device structure, the hole mobilities measured using the SCLC method were 3.7 × 10^{-4}, 2.7 × 10^{-4}, and 2.9 × 10^{-4} cm^2 V^{-1} s^{-1}, respectively. These results are consistent with the result of 3.1 × 10^{-4} cm^2 V^{-1} s^{-1} obtained for the control P3HT:PCBM sample. In contrast to the similar hole mobilities of P3HT:ICMA, P3HT:ICBA and P3HT:ICTA, there were significant differences in the electron mobilities of the various fullerene derivatives, especially between that of ICTA and the others. The current density−voltage (J−V) characteristics of the electron-only P3HT:PCBM/ICMA/ICBA/ICTA blend devices are shown in Figure 5.

To compare the electron mobilities of different P3HT blends with ICMA, ICBA and ICTA, electron-only devices with the ITO/CS_2CO_3/blend/LiF/Al structure were fabricated. It is known that the ITO/CS_2CO_3 bilayer effectively blocks hole injection to the active layer.[34] The thickness of each sample was approximately 100 to 110 nm. Table 3 summarizes the hole and electron mobilities of the PCBM, ICMA, ICBA and ICTA blends with P3HT. The dark current of the P3HT/ICBA device was similar to that of the devices with one solubilizing group (P3HT:PCBM and P3HT:ICMA) . In contrast, the

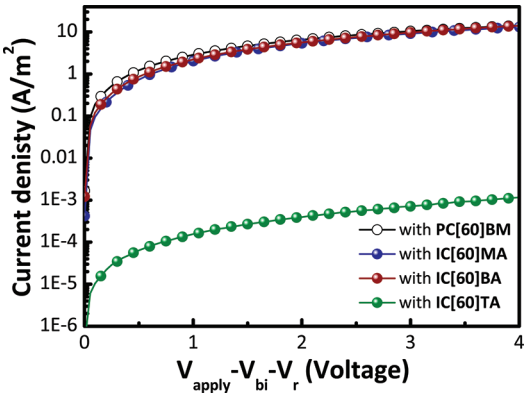

Figure 5. Measured space-charge-limited $J-V$ characteristics of the P3HT:PCBM/ICMA/ICBA/ICTA blend devices under dark conditions for electron-only devices.

Table 3. Calculated Hole and Electron Mobility Values and Electron-Hole Mobility Ratio (SCLC Method)

blend system	hole-only device (μ_h) [cm^2/(V s)]	electron-only device (μ_e) [cm^2/(V s)]	μ_h/μ_e
P3HT:PCBM (1:1)	3.1×10^{-4}	2.3×10^{-4}	1.4
P3HT:ICMA (1:1)	3.7×10^{-4}	2.5×10^{-4}	1.5
P3HT:ICBA (1:1)	2.7×10^{-4}	2.7×10^{-4}	1.0
P3HT:ICTA (1:1)	2.9×10^{-4}	5.0×10^{-7}	5.8×10^{2}

addition of a further indene group in the P3HT:ICTA fullerene resulted in reduction of the electron mobility by 2 orders of magnitude. This result is consistent with previous findings for devices using tris-PCBM[24,31] and probably results from an increase in disorder in the fullerene phase caused by the addition of the solubilizing group and the presence of a greater number of isomers of the trisadduct, both of which prevent efficient packing between the fullerenes and decrease electron transport through the fullerene phase.

The parameter that represents the ratio of the hole-to-electron mobilities (μ_h/μ_e) in the polymer/acceptor blends is crucial to understanding the optoelectronic properties of BHJ solar cells. Therefore, the μ_h/μ_e values of the devices were calculated and compared; the results are summarized in Table 3. Whereas P3HT:PCBM, P3HT:ICMA, and P3HT:ICBA exhibited relatively well-balanced μ_h/μ_e values, the P3HT:ICTA device showed an unbalanced ratio of μ_h/μ_e ($\sim 5.8 \times 10^2$) because of its lower electron mobility. It is known that balanced charge-carrier transport is an important factor for increasing the fill factor in BHJ solar cells.[42,43]

When the charge transport in the device is largely unbalanced, as it was found to be for P3HT:ICTA, charge accumulation can occur in the device, and the photocurrent can then be space-charge-limited. When this occurs, the photocurrent is governed by a square-root dependence on the bias, and a high FF (above 42%) is difficult to achieve.[42,43] However, when the carrier transport is well-balanced, such as for P3HT:PCBM, P3HT:ICMA and P3HT:ICBA, the photocurrent is not limited by space-charge effects, and relatively high fill factors can be achieved. Therefore, we suggest that in addition to the decreased light absorption of the P3HT/ICTA device, as shown in Figure 4, the unbalanced μ_h/μ_e value could provide an additional explanation for the lower current and fill factor of the P3HT/ICTA device than those of the P3HT/ICBA device.

CONCLUSIONS

In summary, we have synthesized a series of indene fullerene derivatives (ICMA, ICBA and ICTA) with different numbers of indene solubilizing groups and investigated the effects of their molecular structure on the performance of BHJ solar cells. An increase in the number of solubilizing groups in the fullerenes was found to increase the LUMO level. Because of their higher LUMO levels, BHJ-type PSCs consisting of P3HT:ICMA, P3HT:ICBA and P3HT:ICTA showed increased V_{oc} values of 0.65, 0.83, and 0.92 V, respectively. Interestingly, the use of ICTA as an electron acceptor produced a further increase in the V_{oc}, to more than 0.9 V. However, despite its high V_{oc} value, the P3HT:ICTA device exhibited a lower PCE (1.56%) than those of the P3HT:PCBM, P3HT:ICMA, and P3HT:ICBA devices because of its lower current and fill factor. The lower current and fill factor can be explained by blue-shifting, as well as the decreased intensity of the vibronic peaks in the UV–vis absorption spectrum and the unbalanced μ_h/μ_e value of the P3HT:ICTA blend; all of these effects are probably caused by the presence of isomers of the ICTA molecule, which affect the charge transport properties of the material. We have successfully demonstrated that a series of indene-fullerene multiadducts can provide a model system for investigating the effects of the number of solubilizing groups on the LUMO and HOMO levels of fullerene derivatives and their performance in BHJ devices. This approach could be extended to other polymer systems that suffer from low V_{oc} because of high LUMO/HOMO levels.

ASSOCIATED CONTENT

Supporting Information

Characterization data including MALDI-TOF mass spectra and ^{1}H NMR. This material is available free of charge via the Internet at http://pubs.acs.org.

AUTHOR INFORMATION

Corresponding Author

*E-mail: bumjoonkim@kaist.ac.kr (B.J.K.); yoonsch@krict.re.kr (S.C.Y.). Phone: 82-42-350-3935 (B.J.K.); 82-42-860-7203 (S.C.Y.).

Author Contributions

‡These authors contributed equally to this work.

ACKNOWLEDGMENTS

This research was supported by the Korea Research Foundation Grant funded by the Korean Government (2011-0030387, 2011-0002124, 2011-0010412), and the EEWS Research Project of the Office of the KAIST EEWS Initiative (EEWS-2010-N01100039). This research was also supported by the New & Renewable Energy KETEP Grant (2010-T100100460) and the Fundamental R&D Program Grant for Core Technology of Materials funded by the Ministry of Knowledge Economy, Republic of Korea.

REFERENCES

(1) Krebs, F. C. *Sol. Energy Mater. Sol. Cells* **2009**, *93*, 394.
(2) Günes, S.; Neugebauer, H.; Sariciftci, N. S. *Chem. Rev.* **2007**, *107*, 1324.

(3) Arias, A. C.; MacKenzie, J. D.; McCulloch, I.; Rivnay, J.; Salleo, A. *Chem. Rev.* **2010**, *110*, 3.
(4) Brabec, C. J.; Sariciftci, N. S.; Hummelen, J. C. *Adv. Funct. Mater.* **2001**, *11*, 15.
(5) Li, G.; Shrotriya, V.; Huang, J.; Yao, Y.; Moriarty, T.; Emery, K.; Yang, Y. *Nat. Mater.* **2005**, *4*, 864.
(6) Ma, W.; Yang, C.; Gong, X.; Lee, K.; Heeger, A. J. *Adv. Funct. Mater.* **2005**, *15*, 1617.
(7) Woo, C. H.; Thompson, B. C.; Kim, B. J.; Toney, M. F.; Fréchet, J. M. J. *J. Am. Chem. Soc.* **2008**, *130*, 16324.
(8) Kim, B. J.; Miyamoto, Y.; Ma, B. W.; Fréchet, J. M. J. *Adv. Funct. Mater.* **2009**, *19*, 2273.
(9) Piliego, C.; Holcombe, T. W.; Douglas, J. D.; Woo, C. H.; Beaujuge, P. M.; Fréchet, J. M. J. *J. Am. Chem. Soc.* **2010**, *132*, 7595.
(10) Chu, T.-Y.; Lu, J.; Beaupré, S.; Zhang, Y.; Pouliot, J.-R. m.; Wakim, S.; Zhou, J.; Leclerc, M.; Li, Z.; Ding, J.; Tao, Y. *J. Am. Chem. Soc.* **2011**, *133*, 4250.
(11) Price, S. C.; Stuart, A. C.; Yang, L.; Zhou, H.; You, W. *J. Am. Chem. Soc.* **2011**, *133*, 4625.
(12) Zhou, H.; Yang, L.; Stuart, A. C.; Price, S. C.; Liu, S.; You, W. *Angew. Chem., Int. Ed.* **2011**, *50*, 2995.
(13) Ong, K.-H.; Lim, S.-L.; Tan, H.-S.; Wong, H.-K.; Li, J.; Ma, Z.; Moh, L. C. H.; Lim, S.-H.; de Mello, J. C.; Chen, Z.-K. *Adv. Mater.* **2011**, *23*, 1409.
(14) Liang, Y. Y.; Feng, D. Q.; Wu, Y.; Tsai, S. T.; Li, G.; Ray, C.; Yu, L. P. *J. Am. Chem. Soc.* **2009**, *131*, 7792.
(15) Park, S. H.; Roy, A.; Beaupre, S.; Cho, S.; Coates, N.; Moon, J. S.; Moses, D.; Leclerc, M.; Lee, K.; Heeger, A. J. *Nat. Photonics* **2009**, *3*, 297.
(16) Chen, H.-Y.; Hou, J.; Zhang, S.; Liang, Y.; Yang, G.; Yang, Y.; Yu, L.; Wu, Y.; Li, G. *Nat. Photonics* **2009**, *3*, 649.
(17) Huo, L.; Zhang, S.; Guo, X.; Xu, F.; Li, Y.; Hou, J. *Angew. Chem., Int. Ed.* **2011**, *50*, 9697.
(18) Moulé, A. J.; Tsami, A.; Bünnagel, T. W.; Forster, M.; Kronenberg, N. M.; Scharber, M.; Koppe, M.; Morana, M.; Brabec, C. J.; Meerholz, K.; Scherf, U. *Chem. Mater.* **2008**, *20*, 4045.
(19) Zhou, E.; Nakamura, M.; Nishizawa, T.; Zhang, Y.; Wei, Q.; Tajima, K.; Yang, C.; Hashimoto, K. *Macromolecules* **2008**, *41*, 8302.
(20) Perzon, E.; Zhang, F.; Andersson, M.; Mammo, W.; Inganäs, O. *Adv. Mater.* **2007**, *19*, 3308.
(21) Brabec, C. J.; Cravino, A.; Meissner, D.; Sariciftci, N. S.; Fromherz, T.; Rispens, M. T.; Sanchez, L.; Hummelen, J. C. *Adv. Funct. Mater.* **2001**, *11*, 374.
(22) Lenes, M.; Wetzelaer, G.-J. A. H.; Kooistra, F. B.; Veenstra, S. C.; Hummelen, J. C.; Blom, P. W. M. *Adv. Mater.* **2008**, *20*, 2116.
(23) Ross, R. B.; Cardona, C. M.; Guldi, D. M.; Sankaranarayanan, S. G.; Reese, M. O.; Kopidakis, N.; Peet, J.; Walker, B.; Bazan, G. C.; Van Keuren, E.; Holloway, B. C.; Drees, M. *Nat. Mater.* **2009**, *8*, 208.
(24) Lenes, M.; Shelton, S. W.; Sieval, A. B.; Kronholm, D. F.; Hummelen, J. C.; Blom, P. W. M. *Adv. Funct. Mater.* **2009**, *19*, 3002.
(25) Kim, K.-H.; Kang, H.; Nam, S. Y.; Jung, J.; Kim, P. S.; Cho, C.-H.; Lee, C.; Yoon, S. C.; Kim, B. J. *Chem. Mater.* **2011**, *23*, 5090.
(26) Voroshazi, E.; Vasseur, K.; Aernouts, T.; Heremans, P.; Baumann, A.; Deibel, C.; Xue, X.; Herring, A. J.; Athans, A. J.; Lada, T. A.; Richter, H.; Rand, B. P. *J. Mater. Chem.* **2011**, *21*, 17345.
(27) Laird, D. W.; Stegamat, R.; Richter, H.; Vejins, V.; Scott, L.; Lada, T. A., Patent WO 2008/018931 A2.
(28) He, Y.; Chen, H.-Y.; Hou, J.; Li, Y. *J. Am. Chem. Soc.* **2010**, *132*, 1377.
(29) Zhao, G.; He, Y.; Li, Y. *Adv. Mater.* **2010**, *22*, 4355.
(30) He, Y.; Zhao, G.; Peng, B.; Li, Y. *Adv. Funct. Mater.* **2010**, *20*, 3383.
(31) Faist, M. A.; Keivanidis, P. E.; Foster, S.; Wobkenberg, P. H.; Anthopoulos, T. D.; Bradley, D. D. C.; Durrant, J. R.; Nelson, J. *J. Polym. Sci., Part B: Polym. Phys.* **2011**, *49*, 45.
(32) Choi, J. H.; Son, K.-I.; Kim, T.; Kim, K.; Ohkubo, K.; Fukuzumi, S. *J. Mater. Chem.* **2010**, *20*, 475.
(33) Puplovskis, A.; Kacens, J.; Neilands, O. *Tetrahedron Lett.* **1997**, *38*, 285.
(34) Lee, J. M.; Park, J. S.; Lee, S. H.; Kim, H.; Yoo, S.; Kim, S. O. *Adv. Mater.* **2011**, *23*, 629.
(35) Chang, Y. T.; Hsu, S. L.; Chen, G. Y.; Su, M. H.; Singh, T. A.; Diau, E. W. G.; Wei, K. H. *Adv. Funct. Mater.* **2008**, *18*, 2356.
(36) Cho, C.-H.; Kang, H.; Kang, T. E.; Cho, H.-H.; Yoon, S. C.; Jeon, M.-K.; Kim, B. J. *Chem. Commun.* **2011**, *47*, 3577.
(37) Gadisa, A.; Svensson, M.; Andersson, M. R.; Inganas, O. *Appl. Phys. Lett.* **2004**, *84*, 1609.
(38) Kim, Y.; Cook, S.; Tuladhar, S. M.; Choulis, S. A.; Nelson, J.; Durrant, J. R.; Bradley, D. D. C.; Giles, M.; McCulloch, I.; Ha, C.-S.; Ree, M. *Nat. Mater.* **2006**, *5*, 197.
(39) Kang, H.; Lee, C.; Yoon, S. C.; Cho, C. H.; Cho, J.; Kim, B. J. *Langmuir* **2010**, *26*, 17589.
(40) Kim, H. J.; Han, A.-R.; Cho, C.-H.; Kang, H.; Cho, H.-H.; Lee, M. Y.; Fréchet, J. M. J.; Oh, J. H.; Kim, B. J. *Chem. Mater.* **2011**, DOI: 10.1021/cm203058p.
(41) Yun, M. H.; Kim, G. H.; Yang, C.; Kim, J. Y. *J. Mater. Chem.* **2010**, *20*, 7710.
(42) Mihailetchi, V. D.; Xie, H. X.; de Boer, B.; Koster, L. J. A.; Blom, P. W. M. *Adv. Funct. Mater.* **2006**, *16*, 699.
(43) Blom, P. W. M.; Mihailetchi, V. D.; Koster, L. J. A.; Markov, D. E. *Adv. Mater.* **2007**, *19*, 1551.